ELSEVIER

Chemical Geology 185 (2002) 241–254

CHEMICAL GEOLOGY
INCLUDING
ISOTOPE GEOSCIENCE

www.elsevier.com/locate/chemgeo

Temporal changes in the lead isotopic composition of red clays: comparison with ferromanganese crust records

L.V. Godfrey [a,b,*]

[a] *Department of Geological Sciences, Snee Hall, Cornell University, Ithaca, NY 14853, USA*
[b] *Department of Earth Sciences, Cambridge University, Downing Street, Cambridge CB2 3EQ, UK*

Received 12 May 2000; accepted 25 October 2001

Abstract

A record of changes in Pb and Sr isotopic composition of two cores (DSDP 86 576A and LL44 GPC3) from the red clay region of the central North Pacific has been determined for the past 60–65 million years. The isotope records of the eolian silicate fraction of the red clays reflect the change in source area as the core sites migrated under different wind systems. The Sr isotope compositions of eolian silicate material are consistent with Asian loess and North American arc volcanism that has been recognized from mineralogical studies. The silicate-bound eolian Pb isotopic compositions similarly reflect Asian loess and arc volcanism. The isotope records of three ferromanganese crusts from similar locations in the central Pacific are similar to the eolian component of red clays, but offset to less radiogenic values. This may be due to two mechanisms: (1) Pb that can be removed from eolian material by seawater is much less radiogenic, or less likely (2) hydrothermal Pb can be transported further away from venting sites through particle exchange with seawater, despite hydrothermal venting acting as a *net* sink of oceanic Pb. The temporal changes in Pb isotopes in the ferromanganese crusts, bulk red clays and eolian silicates are similar although offset from each other suggesting that eolian deposition is an important source of Pb to seawater and to ferromanganese crusts. This contrasts with the Atlantic and Southern Ocean where more intense deep water flow leads to isotopic gradients in FeMn crusts that do not reflect surface water conditions immediately above the crust. A mechanism is proposed which accounts for Pacific deepwater Pb being isotopically influenced by eolian deposition.

Keywords: Lead isotopes; Strontium isotopes; Red clays; North Pacific

1. Introduction

In comparison to seawater records of elements that have long ocean residence times such as Sr and Os (e.g. Hess et al., 1986; Peucker-Ehrenbrink et al., 1995), the seawater records of elements with short residence times (comparable to ocean ventilation rates) are more complex because they are affected by changes in both sources and mixing relative to input and removal rates. Recent studies using lead isotopes in ferromanganese crusts hypothesize that the main cause of temporal variations in Pb isotopes recorded is changes in oceanic circulation patterns. This theory has been further developed with the suggestion that circulation changes result from changes in paleogeog-

* Department of Earth and Environmental Sciences, Williams Hall, Lehigh University, Bethlehem, PA 18015, USA.
E-mail address: lig5@lehigh.edu (L.V. Godfrey).

0009-2541/02/$ - see front matter
PII: S0009-2541(01)00406-5

raphy such as the closing of the Panama Isthmus and the Tethys Ocean (Ling et al., 1997; Burton et al., 1997; Christensen et al., 1997; O'Nions et al., 1998), with additional modifications arising from changes in climate (Christensen et al., 1997). The records of seawater ε_{Nd} and Pb isotopes from FeMn crusts in the NW Atlantic both show the increasing influence of a radiogenic water mass starting about 9.1 Ma (Burton et al., 1997; O'Nions et al., 1998). On the other hand, there is little similarity between the ε_{Nd} and Pb isotope records in samples from the Indian and Pacific Oceans (Ling et al., 1997; Christensen et al., 1997; O'Nions et al., 1998). The lack of correlation between Pb and Nd isotope records from ferromanganese crusts in the Indian and Pacific Oceans has yet to be fully explained. This study addresses the controls on Pb isotope compositions of ferromanganese crusts by comparison to Pb isotope records from red clays that contain a mixture of eolian and seawater Pb.

Interpretation of Pb isotope records is particularly complicated because the modern budget of 'natural' Pb in the oceans is poorly constrained. It is known that hydrothermal vent fluids have very high concentrations of Pb, but the majority of vent fluid lead is first sequestered in sulfides with further scavenging of dissolved Pb by hydrothermal particles in buoyant and neutrally buoyant plumes (Godfrey et al., 1994). Scavenging of dissolved Pb is also thought to occur in rivers and estuaries with the result that the majority of riverine Pb, if not all, is removed from solution and does not contribute to reservoir of Pb in the open ocean (Elbaz-Poulichet et al., 1984; Hamelin et al., 1990). However, it has also been postulated that a major source of Pb to the oceans is from partial dissolution of riverine particulates (von Blanckenburg et al., 1996). Young volcanic arcs and margins are important sources of particulate material to the Pacific Ocean (Milliman and Syvitski, 1992) and this could also be a significant source of dissolved Pb. An alternative mechanism of introducing arc Pb to seawater is through dissolution of mineralogically unstable tephra in marginal areas of the Pacific (Straub and Schmincke, 1998).

Ferromanganese crusts acquire Pb from seawater and any Pb-containing particles that adhere to their surfaces. Chow and Patterson (1962) and other workers have shown that slowly accumulating sediments such as red clays also acquire most of their Pb from seawater. The non-seawater Pb in these sediments is located in detrital minerals which, in the distal areas of the Pacific, are transported by the wind (Rea, 1994). Measurements of seawater Pb isotopes in the Pacific indicate that in remote areas, surface seawater Pb is eolian, and fluvial Pb inputs are only important in coastal areas (Flegal et al., 1986). However, eolian Pb in the modern ocean may be important because anthropogenic Pb is largely eolian and is thought to be more soluble than natural Pb. Since the isotope records preserved by red clays is a combination of both eolian and seawater isotope variations, the relative importance of either source depends on sediment accumulation rates and the length of time sediments have been in contact with seawater. Two well-characterized cores are used in this study, LL44 GPC3 and DSDP 86 site 576A. The sedimentation history and sources of material to GPC3 have been studied using a combination of concentration distributions and partitioning models (Leinen, 1987; Kyte et al., 1993) and the isotope variations are considered in this existing framework. Using the conclusions about the sources of Pb to these two cores, three ferromanganese crust records from the Pacific (Ling et al., 1997; Christensen et al., 1997) are reinterpreted.

2. Samples

The locations of GPC3, 576A and the three ferromanganese crusts are shown in Fig. 1. The 23.5-m core LL44 GPC3 (30°19.9′ N, 157°49.9′ W; 5705 m depth) and 52.8-m core DSDP 86 site 576A (32°21.4′ N, 164°16.5′ E; 6217 m depth), both from the central North Pacific, represent roughly continuous sedimentation through the Cenozoic based on ichthyolith stratigraphy (Doyle, 1980; Doyle and Riedel, 1979, 1985). Accumulation rates before 4 Ma varied between 15 and 70 g/cm^2/Ma in 576A (Doyle, 1980; Doyle and Riedel, 1979, 1985) and between 5 and 70 g/cm^2/Ma in GPC3. The sediment accumulation rates during the Paleocene were generally higher than the rates for the rest of the Cenozoic with the exception of the last 4 Ma. With increasing aridity in the northern hemisphere, and the eventual onset of glaciation at 4 Ma, sediment accumulation rates in both cores increase dramatically to about 720 g/cm^2/Ma in 576A and 190 g/cm^2/Ma in GPC3 (Janecek, 1985; Kyte et al.,

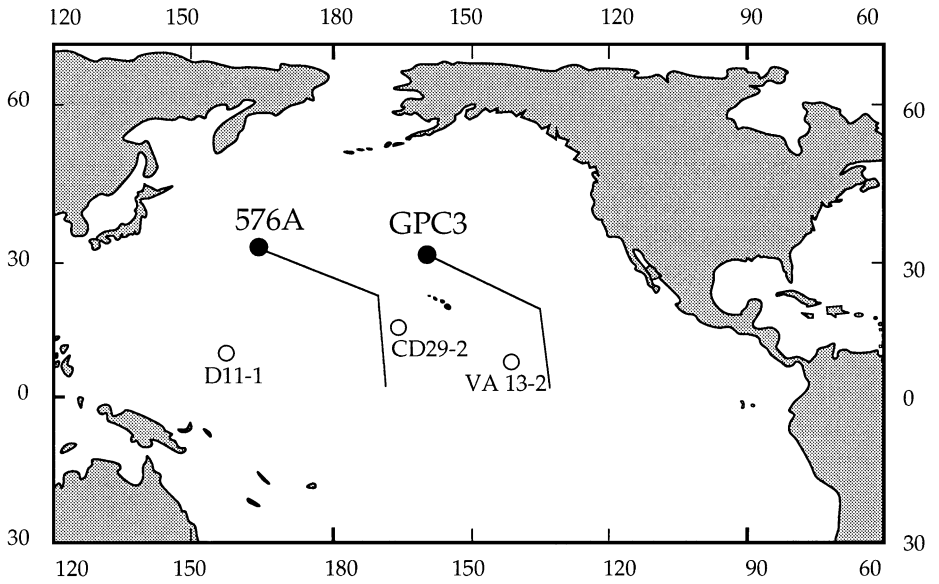

Fig. 1. Sample location of cores and ferromanganese crusts. The backtrack paths of LL44 GPC3 and site 576A according to the plate rotation model of Van Andel et al. (1975) are shown. 20°N is the approximate boundary between Northern hemisphere westerlies and northeast tradewinds.

1993). Stratigraphic resolution in the slowest accumulating section of both cores is about 5 Ma, and <0.1 Ma in the fastest accumulating sections. The Cretaceous Tertiary boundary is defined by high Ir concentrations (Kyte and Wasson, 1986).

The Pb isotope records from three ferromanganese crusts have been published by Ling et al. (1997) and Christensen et al. (1997). Briefly, the crusts were collected from seamounts at different depths in the Central Pacific. The lower portions of the crusts CD29-2 (below 40 mm) and D11-1 (45 mm) have been phosphatized. During phosphatization processes, Pb is transferred into an apatite phase from Fe–Mn oxides (Koschinsky and Halbach, 1995). Although it does not appear that the apatite phases bring additional Pb to the original non-phosphatized crust (Koschinsky and Halbach, 1995), it is possible that redistribution of Pb influences the isotope record.

3. Methods

Unwashed samples were ground in agate and dissolved in open PTFE beakers using distilled HF, HNO_3 and HCl digestions. Some samples were also leached overnight with 6 M HCl and rinsed with 6 M HCl to remove all Sr and Pb associated with the hydrogenous Fe–Mn phases. Initially, 1.75 M HCl was used as the leach, but the acid residues had high Fe, Mn, Co, Ni, Cu and Zn concentrations suggesting that not all the ferromanganese phases had been dissolved. Since it was important to remove all seawater-derived Sr and Pb, a higher concentration acid (6 M HCl) was favored, although dissolution of some detrital clays was inevitable. The concentrations of major and most trace elements were measured by ICP-AES using external standards at the NERC facility of Dr. J. Walsh. Lead, U and Th were measured by ICPMS (VG Elemental PQ I) using external standards at Surrey University. Strontium isotope ratios were measured using a single collector Micromass 54E mass spectrometer at Cambridge University, and measurements of NBS 987 ran during the period of data acquisition gave 0.71022. Isotopic measurements of Pb were also made using either the Cambridge 54E or the Micromass Sector 54 at Cornell University using a four-cup static routine. Procedural Pb blanks were between 50 and 250 pg, which comprised $<1‰$ of the total analyte. Twenty

NBS 981 standards measured during the periods of data acquisition gave values of $^{206}Pb/^{204}Pb = 16.914 \pm 0.018$, $^{207}Pb/^{204}Pb = 15.462 \pm 0.010$, $^{208}Pb/^{204}Pb = 36.615 \pm 0.035$ and were corrected to values of $^{206}Pb/^{204}Pb = 16.937$, $^{207}Pb/^{204}Pb = 15.491$, $^{208}Pb/^{204}Pb = 36.704$ (Hamelin et al., 1990).

4. Results

4.1. Lead and lead isotope distribution

The range in Pb concentrations for both cores, 25–90 ppm (see Appendix A), is typical of pelagic clays (~ 70 ppm; Cronan, 1976). In GPC3, the Pb concentration at the start of the Cenozoic is between 37 and 50 ppm, increases to a maximum of 90 ppm between 52 and 45 Ma, and then decreases to about 27 ppm by the end of the Cenozoic. This decrease in Pb concentration is punctuated by low concentrations that coincide with an altered ash layer. The variation in Pb concentrations is most similar to Mn (GPC3 $r^2 = 0.86$; 576A $r^2 = 0.59$), an observation also made by Kyte et al. (1993). The Pb concentration in core 576A sediments is more uniform, 22–58 ppm, and the down-core variation does not exhibit any distinct temporal patterns, nor does it resemble the Mn distribution. The depth distribution of Pb and Mn concentrations do not correlate strongly with Fe or other elements indicative of hydrothermal sedimentation in GPC3 or in 576A (Kyte et al., 1993).

The range in Pb isotopes in the two cores is similar to the range in ferromanganese crusts formed during the past 60 Ma in the central Pacific (Ling et al., 1997): $^{206}Pb/^{204}Pb = 18.55–18.76$; $^{207}Pb/^{204}Pb = 15.57–15.69$; $^{208}Pb/^{204}Pb = 38.41–38.97$. The Pb isotopic composition of red clays, ferromanganese crusts and metalliferous sediments in the Pacific Ocean form mixing arrays between MOR basalts and continental crust on Pb–Pb isotope plots (Fig. 2). The isotope arrays described by the three ferromanganese crusts overlap each other, although VA13-2 tends to plot to lower $^{208}Pb/^{204}Pb$ than D11-1 or CD29-2 for a given $^{206}Pb/^{204}Pb$. The field for metalliferous sediments associated with the EPR encompasses data for the ferromanganese crusts, but extends with lower $^{206}Pb/^{204}Pb$ towards the field for Pacific MORB (Chen et al., 1987; Ito et al., 1987; Hegner and Tatsumoto, 1987). Turbidites from the eastern North Pacific plot parallel to the field for MORB, but with higher $^{208}Pb/^{204}Pb$ (Hemming and McLennan, 2001). The array formed by turbidites from the western North Pacific is also parallel to Pacific MORB, but to even higher $^{208}Pb/^{204}Pb$ (Hemming and McLennan, 2001). This array includes Asian loess, its acetic acid soluble component and silicate fraction (Jones et al., 2000). The majority of samples from core GPC3 plot on top of the ferromanganese crust isotope fields and overlap with eastern Pacific turbidites. The samples from GPC3 deposited between 34 and 52 Ma have elevated $^{208}Pb/^{204}Pb$ compared to the rest of the core. All samples from core 576A plot above the ferromanganese arrays, and are compositionally similar to the samples from GPC3 deposited between 34 and 52 Ma. Most of the samples from 576A overlap the western Pacific turbidite/Asian loess isotope fields.

The silicate fraction of red clays of both cores plot to higher $^{206}Pb/^{204}Pb$ and $^{208}Pb/^{204}Pb$ than the bulk clays (Fig. 2). In general, detrital silicates from 576A have higher $^{208}Pb/^{204}Pb$ for a given $^{206}Pb/^{204}Pb$ compared to detrital silicates from GPC3. The exception are samples from GPC3 deposited during the last 20 Ma that fall on top of the 576A samples in the Pb–Pb isotope plot. These two samples and all of 576A plot between bulk Asian loess and its silicate fraction (Jones et al., 2000). The other samples from GPC3 deposited before 20 Ma form an array that extends the bulk red clay array towards coastal Oregon greywackes (Church, 1976). Turbidites deposited along the Mexican coast that might contain some of the volcanoclastic rocks categorized as ‘‘andesitic eolian 2’’ by Kyte et al. (1993) form a less radiogenic continuation of the older than 20 Ma array of GPC3. Since the silicate fraction of GPC3 plots towards more radiogenic lead compared to bulk red clays, western Mexican volcanism as a major source of Pb to GPC3 is questionable.

The down-core variation in $^{206}Pb/^{204}Pb$ ratios in core GPC3 generally parallels the data from crust VA13-2, but is offset to more radiogenic values (Fig. 3a). The biggest discrepancy between the isotope records of GPC3 and VA13-2 occurs as a spike toward more radiogenic Pb isotope ratios in the red clay between 28 and 36 Ma. This increase to more radiogenic Pb compositions may be due to an altered ash layer deposited between 36 and 22 Ma (13–9.5 m) in this

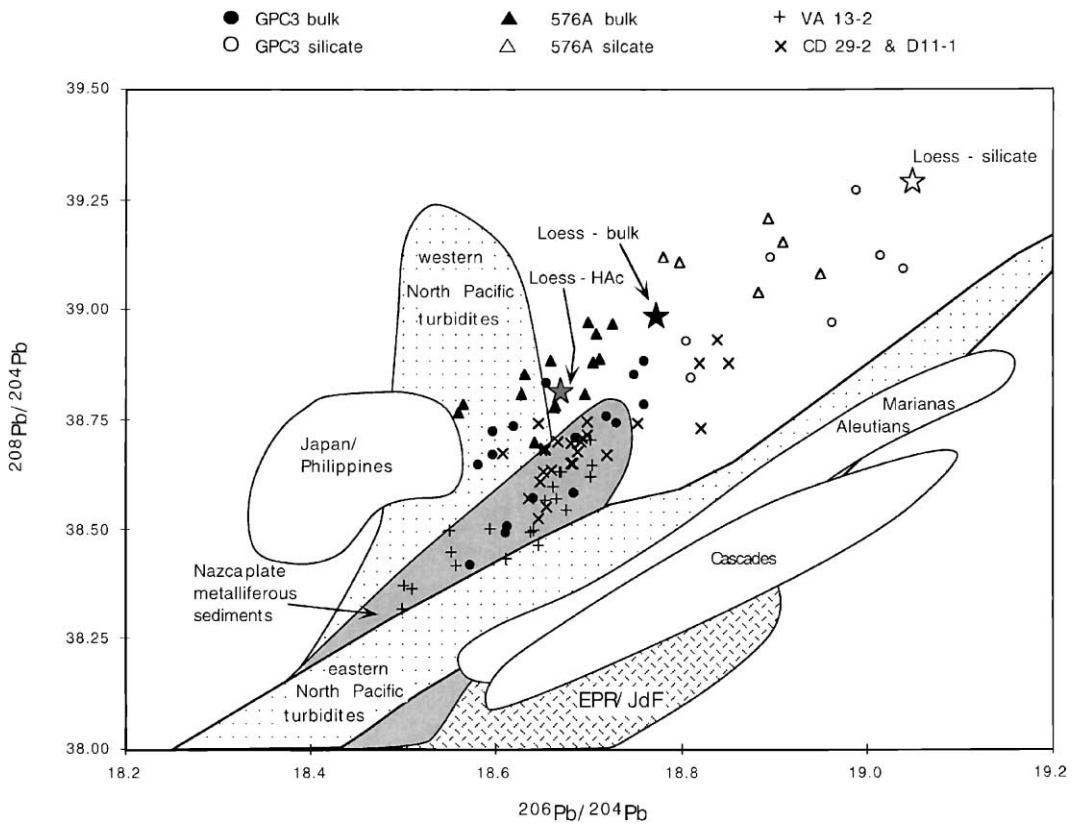

Fig. 2. $^{208}Pb/^{204}Pb-^{206}Pb/^{204}Pb$ plot of the cores and ferromanganese crusts (data from Ling et al., 1997) used in this study. Nazca plate metalliferous sediments from Dasch (1981), Juan de Fuca Ridge and Gorda Ridge (JFR-GR) field from Hegner and Tatsumoto (1987) combined with the EPR field from Ito et al. (1987) and Chen et al. (1987), Cascades from Church (1976) and various volcanic arcs around the Pacific rim (Sun, 1980). The composition of Asian loess (bulk, silicate and acetic acid soluble phase) is included (Jones et al., 2000). Metalliferous sediments closest to the EPR and in the Bauer Deep show incorporation of mantle Pb through coprecipitation and adsorption on Fe and Mn oxides and hydroxides.

section. The down-core trend in $^{208}Pb/^{204}Pb$ is also similar to that in VA13-2 except for the section deposited between 52 and 28 Ma, where the red clays have much higher $^{208}Pb/^{204}Pb$. This section of GPC3 has high accumulation rates of hydrothermal material and silicic volcanic material (Kyte et al., 1993). The temporal variation of the isotopic composition of the silicate fraction of GPC3 also parallels VA13-2 but is considerably more radiogenic in $^{206}Pb/^{204}Pb$ and $^{208}Pb/^{204}Pb$. The excursion to even higher $^{206}Pb/^{204}Pb$ and $^{208}Pb/^{204}Pb$ is more limited to the altered ash layer than it was for the bulk sediment. The offset in Pb isotope ratios between 576A and D11-1 and CD29-2 (Fig. 3b) for sediments deposited before 30 Ma is to less radiogenic Pb in red clays for $^{206}Pb/^{204}Pb$ but to more radiogenic $^{207}Pb/^{204}Pb$ and $^{208}Pb/^{204}Pb$ ratios. After 30 Ma, $^{206}Pb/^{204}Pb$ ratios are more radiogenic in core 576A than in either crust, and the offset to more radiogenic $^{207}Pb/^{204}Pb$ and $^{208}Pb/^{204}Pb$ increases. However, it should be noted that the deeper sections of D11-1 and CD29-2 are phosphatized. The effect of phosphatization on Pb and Pb isotopes is not fully understood (Koschinsky et al., 1997). The silicate fraction of 576A is always more radiogenic than the crusts. The similarity in the trend between the silicate, bulk clay and crusts is strong for $^{206}Pb/^{204}Pb$ ratios, but is weaker between 60 and 25 Ma for $^{208}Pb/^{204}Pb$. This corresponds to the phosphatized sections of the crusts, and the dissimilarity of the isotope trends may have been caused by this.

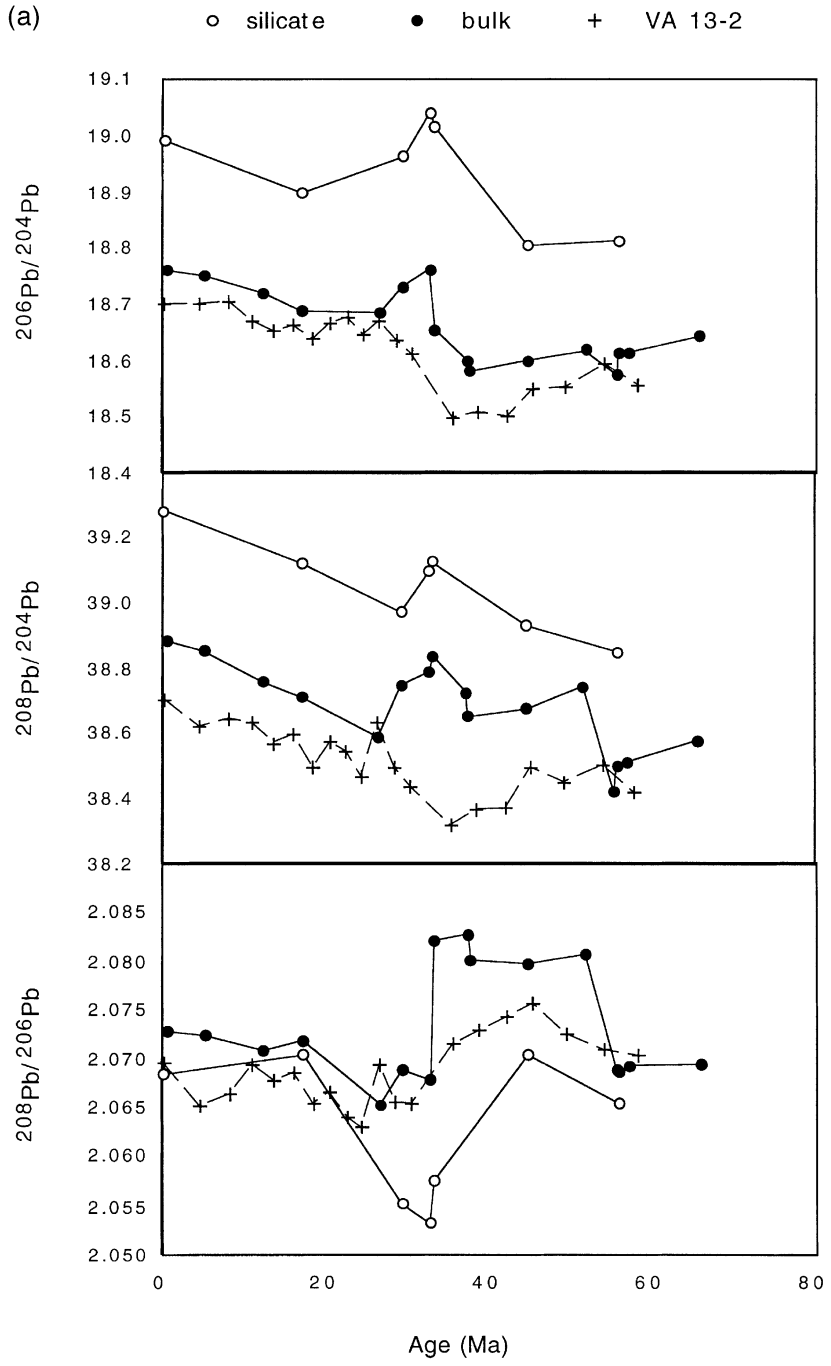

Fig. 3. (a) Variation in $^{206}Pb/^{204}Pb$, $^{208}Pb/^{204}Pb$ and $^{208}Pb/^{206}Pb$ ratios in bulk red clays from GPC3 and nearby ferromanganese crust VA13-2. (b) Variation in $^{206}Pb/^{204}Pb$, $^{208}Pb/^{204}Pb$ and $^{208}Pb/^{206}Pb$ ratios in bulk red clays from 576A and nearby ferromanganese crusts D11-1 and CD29-2.

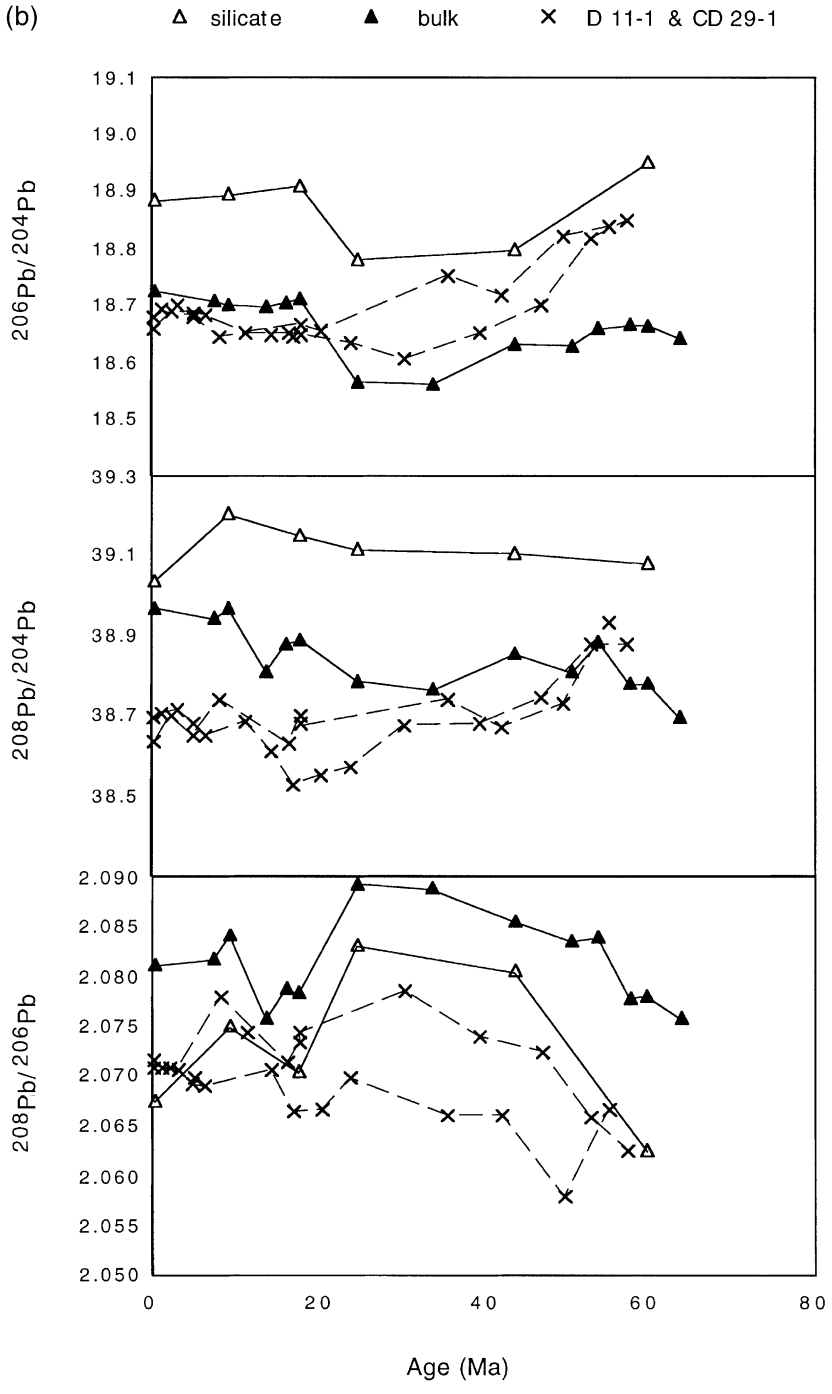

Fig. 3 (*continued*).

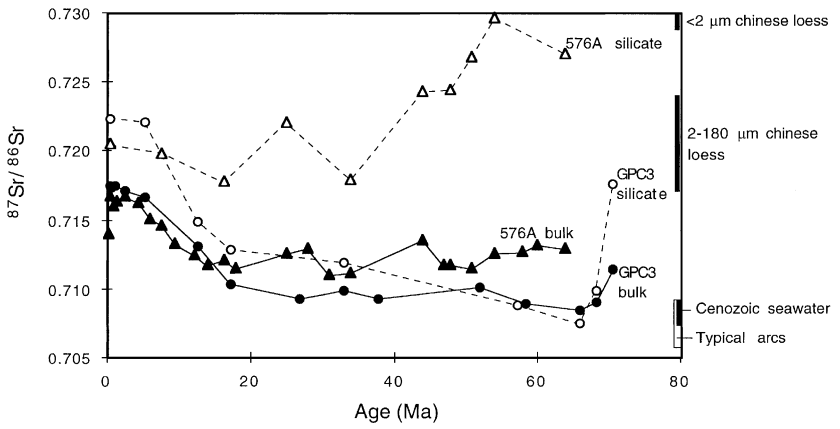

Fig. 4. Variations in $^{87}Sr/^{86}Sr$ of bulk and acid leached sediment as a function of age. The compositions of Cenozoic seawater and loess (bulk and 2- to 20- and <2-μm-size fractions; Asahara, 1999) are included.

4.2. Strontium and strontium isotope distribution

The concentration of Sr in both cores is lowest in most recently deposited sediments and highest in sediments deposited between 60 and 50 Ma (Appendix A). The distribution of Sr is similar to Ca and P (see Appendix A), and reflects the distribution of fish debris (Corliss and Hollister, 1982). There is no calcium carbonate in either core. Variations in the Sr isotopic composition of bulk sediment of both cores through time are similar (Fig. 4). From the beginning of the Cenozoic to the middle Miocene, $^{87}Sr/^{86}Sr$ ratios are relatively uniform, ranging from 0.7084 to 0.7114 in core GPC3 and from 0.7110 to 0.7136 in core 576A. At about 15 Ma, the $^{87}Sr/^{86}Sr$ ratios in both cores increased to between 0.7167 and 0.7174 and by 2.5 Ma, remained high to the present. Changes in the Rb concentrations parallel those of $^{87}Sr/^{86}Sr$ suggesting that it is the proportion and isotopic composition of detrital material that determines the Sr isotopic compositions of the bulk sediment.

The $^{87}Sr/^{86}Sr$ composition of the silicate material, determined from leaching experiments, shows a wider variation than the bulk sediment: from 0.7074 and 0.7223 in core GPC3 and 0.7178 and 0.7300 in core 576A (Fig. 4). While the temporal variation in GPC3 is similar to the bulk sediment, the magnitude and trend of the 576A silicate data are totally different. They show a marked decrease from highly radiogenic values at 50 Ma to about 0.718 at 34 Ma.

The variations of Pb and Sr isotope composition of the silicate material in both cores do not correlate. This contrasts with deep-sea turbidites where there is a general correlation between strontium and lead isotopes (Hemming and McLennan, 2001). The altered ash layer of GPC3, observable in $^{206}Pb/^{204}Pb$ and $^{208}Pb/^{204}Pb$ ratios, is not apparent in the $^{87}Sr/^{86}Sr$. Likewise, the addition of material in 576A with very radiogenic Sr isotope ratios, presumably old crustal material, is not evident from Pb isotope ratios. The greater sensitivity of Pb isotopes towards arc material presumably reflects the different Sr and Pb concentrations of Asian loess and volcanic arc material in the western Pacific.

5. Discussion

5.1. Strontium and lead isotopic compositions of eolian material

Mineralogical studies of the two cores show that they can be described by mixing of two sources: quartz-rich Asian sediment carried by the westerlies and arc-dominated material from North and Central America carried by the tradewinds (Leinen, 1985; Schramm, 1989). Based on quartz content and mass accumulation rates, the core-site backtracks crossed the boundary from the tradewinds into the westerlies between 35 and 30 Ma for GPC3 and between 25 and

15 Ma for 576A (Leinen, 1985). The Sr isotopic composition of silicate material does not clearly show this boundary in either core. The detrital $^{87}Sr/^{86}Sr$ ratios become similar between the two sites only during the last 10 Ma; these ratios match Asian loess (0.720, Asahara et al., 1995; Nakai et al., 1993). Comparison between the distributions of Sr isotopic compositions of surface sediments (Asahara et al., 1995) and the isotopic composition of the bulk sediments along the core backtracks show that the isotopic gradients that exist today in surface sediment compositions have persisted over time scales that precede Northern hemisphere glaciation.

The unradiogenic sediments from core GPC3, deposited between 70 and 35 Ma, also have high Ca/Al ratios (see Appendix B). The proportion of plagioclase in the <63-μm fraction reaches 40% at 22.35 m (about 69 Ma) (Leinen and Heath, 1981); this plagioclase is the most likely reason for low $^{87}Sr/^{86}Sr$ and high Ca/Al. The source of plagioclase-rich material has been suggested as being the western and central American volcanic arc that was particularly active during the mid-Tertiary (Keith, 1978; Kyte et al., 1993), although Pb isotope ratios of silicate material in GPC3 deposited at this time suggest a source further north on the North American Pacific coast (Fig. 2). Based on the core-site position and wind trajectories, core 576A also received material from North America during the first half of the Cenozoic, but the Sr isotopic composition of eolian material is very radiogenic suggesting the source area was old continental crust. Compared to the isotopic compositions of silicate fraction of modern surface sediments in the northern central and northeastern Pacific (Asahara et al., 1995), silicate material in the lower part of 576A is more radiogenic. The $^{87}Sr/^{86}Sr$ and $^{87}Rb/^{86}Sr$ isotopic compositions of modern eolian sediments deposited where 576A was 50–60 Ma indicate the presence of continental material from Asia and arc volcanic material (Asahara et al., 1995), and that fine size fractions are more radiogenic than coarser size fractions (Asahara, 1999). The similarity in the $^{87}Sr/^{86}Sr$ composition of the silicate fraction of 576A with the fine (<2 μm) fraction of Asian continental material (Fig. 4; Asahara, 1999) plus the similarity in lead isotopes of the silicate material and the silicate fraction of Asian loess (Jones et al., 2000) give compelling evidence that throughout the Cenozoic, site 576A remained within the dust plume from Asia. The decrease in quartz content may reflect changes in the dust-carrying capacity of the westerlies, rather than a migration of 576A out of the influence of the NE tradewinds (Leinen, 1985).

5.2. Comparison of silicate eolian and ferromanganese crust Pb isotope compositions

5.2.1. Paleocene to Oligocene

The major difference between the Pb isotope records of silicate material in core GPC3 and ferromanganese crust VA13-2 occurs around 30 Ma (Fig. 3a). At this time, a spike in the lead isotopic composition of eolian material in GPC3 to quite radiogenic $^{208}Pb/^{204}Pb$ ratios (and high $^{208}Pb/^{206}Pb$) is not apparent in VA13-2. Between 60 and 35 Ma, the high $^{208}Pb/^{206}Pb$ of the bulk clay is only weakly reflected in VA13-2 and not at all in the silicate phase. This might imply that since red clays contain lead from seawater and eolian material, the more soluble component of eolian material that has not been directly analysed had very high $^{208}Pb/^{204}Pb$ over this interval; high $^{208}Pb/^{204}Pb$ is also distinctive in the loess data of Jones et al. (2000). Temporal variations in Pb isotope ratios of eolian material in core 576A and ferromanganese crusts D11-1 and CD29-2 are also similar (Fig. 3b). $^{206}Pb/^{204}Pb$ compositions of these ferromanganese crusts are more radiogenic than core 576A bulk sediment before 25–18 Ma but not as radiogenic as the silicate material.

5.2.2. Oligocene to present

During the last 20–35 million years, cores 576A and GPC3 have been positioned under the westerlies and have received eolian material from Asia. Lead incorporated into ferromanganese crusts is consistently less radiogenic than the silicate material, and exhibits lower $^{208}Pb/^{206}Pb$ (Fig. 3a and b). The temporal variations in Pb isotopes during this period are similar between grouped crust and silicate components of red clay cores.

5.3. Sources of Pb to ferromanganese crusts

It is generally assumed that Pb in ferromanganese crusts is derived from seawater in contact with the crust. Since the distribution of Pb isotopes in modern Pacific seawater has not been measured at depths below the thermocline and because the deep Pacific

may be contaminated with anthropogenic Pb, it is currently not possible to verify this assumption. The average oceanic residence time of Pb in the North Pacific is about 80 years which contrasts with its surface residence time of 2 years (Schaule and Patterson, 1981). The ventilation rate of the Pacific is estimated to be slightly less than 1000 years (von Blanckenburg and Igel, 1999) which is considerably longer than the average oceanic residence time of Pb. Low particulate fluxes and low suspended particulate concentrations typical of the central gyres regionally increase residence times of particle reactive elements such as Pa and Pb, and the accumulation rates of ^{231}Pa and ^{210}Pb reflect this (Carpenter et al., 1981; Anderson et al., 1990). Mixing of Pb in deep and intermediate water is reflected in the similar isotopic compositions of the crusts from different areas and depths in the Pacific (Ling et al., 1997).

The similarity of the ferromanganese crust and silicate eolian records suggests that wind-borne dust is an important source of Pb to the central regions of the Pacific, and that the vertical transport of Pb is not obscured by horizontal movement. This contrasts with the Atlantic where more vigorous circulation of intermediate and deep water masses affects both vertical concentration profiles (Boyle et al., 1986) and Pb isotopic compositions of ferromanganese crusts (Burton et al., 1997; O'Nions et al., 1998; Reynolds et al., 1999; Frank et al., 1999). The less radiogenic ratios of the crusts compared to eolian material suggest that the Pb leached from eolian material by seawater is less radiogenic than bulk eolian material. An alternative explanation is that there are additional sources of unradiogenic Pb to seawater.

The three ferromanganese crusts plot between MORB and continental crust on Pb–Pb isotope plots. Christensen et al. (1997) observed that Pacific crusts trend towards MORB compositions, but did not distinguish between a direct hydrothermal origin or a recycled origin in the form of subducted hydrothermal sediments and arc erosion. The ferromanganese crusts do not plot towards arc sources with high ^{208}Pb/^{206}Pb (Jones et al., 2000), and the greatest discrepancy between the crust and eolian record tends to occur where an eolian arc Pb is dominant in bulk red clay compositions. Between 45 and 33.5 Ma, crust VA13-2 trends towards particularly low ^{206}Pb/^{204}Pb and low ^{208}Pb/^{204}Pb, while the eolian component of core GPC3 has higher ^{206}Pb/^{204}Pb and ^{208}Pb/^{204}Pb. The isotopic differences can be explained by the paleolocations of VA13-2 and GPC3. Both the crust and core sites were located under the same wind system, but VA13-2 was closer to the EPR ridge crest than the core site of GPC-3. The location of crust VA13-2 when it acquired its least radiogenic Pb was no further from the ridge axis than modern metalliferous sediments on the Nazca Plate which have equally unradiogenic Pb (Dasch, 1981). There is no requirement for hydrothermal fluxes to have been greater in the past, nor deep circulation to have been more energetic, to account for the more MORB-like Pb isotope composition of crust VA13-2.

Profiles of Pb isotopes in seawater and particulate material in the deep Pacific have not been measured, but until that time, we can use ferromanganese crusts and eolian sources to speculate on the distribution of Pb isotopes. If the scavenging residence time of Pb depends on particle fluxes, as implied by enhanced removal of ^{210}Pb at margins (e.g. Carpenter et al., 1981), it is probable that it is sufficiently long that the Pb isotopic composition of seawater and authigenic material is the same throughout the central North Pacific gyre. The average scavenging rate of Pb is 0.03 pM/year based on a scavenging constant of 1/150 year^{-1} and a deep-water Pb concentration of 5 pM (Schaule and Patterson, 1981) but this may decrease to <0.01 pM/year in the central gyre if the scavenging constant decreases similarly to Pa, for example (Anderson et al., 1990). The range in the scavenging rate of Pb is very similar to the eolian flux [0.06–0.002 pM/year, based on a Pb concentration in eolian dust of 30 ppm (this study) and eolian fluxes of 5–200 μg/cm^2/year (Kyte et al., 1993; Rea and Janecek, 1982)]. The highest scavenging rates coincide with the highest eolian fluxes, but locally, there may exist discrepancies. If the prehistoric Pb concentration of the deep Pacific was lower than 5 pM, then the eolian flux may be larger than the scavenging rate.

The changes in ferromanganese crust isotopic compositions through time coincide with the more pronounced changes in eolian Pb isotope ratios. The similarity of crust and eolian Pb isotope records implies that either crusts contains appreciable quantities of eolian dust that have Pb that can be leached by weak acids (Ling et al., 1997), that there is a bottom source of Pb from sediments into seawater, or that

there is an effective mechanism of transferring eolian dust Pb into deep water. The vertical profile of pollution Pb concentrations indicates that Pb is leached from eolian dust in the surface ocean and is rapidly scavenged by particulate matter in the upper ocean (Schaule and Patterson, 1981; Boyle et al., 1986; Sherrell et al., 1992). Throughout the water column, dissolved and suspended particulate Pb are in isotopic equilibrium, but equilibrium is not established between dissolved and sinking particulate Pb because sinking particles lack the time to fully exchange their Pb (Sherrell et al., 1992). A proportion of deep suspended particles is formed from disaggregation of sinking particles, which may re-aggregate and continue to sink. Disaggregation of surface-formed particles to form deep suspended particles is a mechanism by which surface-water Pb may be transported into the deep ocean and allows the deep ocean to acquire isotopic characteristics of the surface ocean. Thus, the Pb isotopic composition of ferromanganese crusts and deep water may reflect Pb isotopes in surface seawater, which in remote areas of the ocean is strongly influenced by eolian deposition. If equilibrium between suspended particulate and dissolved Pb is an important mechanism through which deep water establishes its isotope composition, then deep water would also be expected to isotopically reflect the depth in the ocean where maximum uptake of Pb on to particles takes place, the surface ocean.

Acknowledgements

This work was funded by NERC funding to H. Elderfield and an NSF grant to Dr. W.M. White (OCE 93-02890). I thank H. Elderfield, G. Ravizza, J. Wu and W. White for many helpful comments and discussion about this study. The manuscript was much improved by comments by C. Jones and Y. Asahara.

Appendix A

Depth, age element and isotope compositions for bulk material in LL44 GPC3

Depth (m)	Age (Ma)	MAR (g/cm^2/Ma)	Pb (ppm)	Fe (wt.%)	Mn (wt.%)	^{206}Pb/^{204}Pb	^{207}Pb/^{204}Pb	^{208}Pb/^{204}Pb	Sr (ppm)	Ca (wt.%)	P (wt.%)	Pb (ppm)	^{87}Sr/^{86}Sr
0.7	0.36	153.67	27	5.39	0.33				151	0.55	0.04	156	0.71741
1.7	0.73	185	26.5	5.34	0.33	18.759	15.645	38.882	152	0.49	0.004	157	0.71736
2.8	1.23	121.78	28	5.41	0.4				150	0.48	0.004	160	0.71740
4.3	2.5	61.3	28	5.39	0.48				153	0.57	0.04	158	0.71708
5.5	5.35	24	26.9	6.02	0.59	18.748	15.643	38.852	168	0.55	0.09	157	0.71662
7	12.5	15	31.9	6.32	0.9	18.718	15.62	38.758	182	0.77	0.13	117	0.71303
8.4	17.2	10	39.6	6.71	1.37	18.685	15.608	38.709	223	1.1	0.2	103	0.71039
10.5	26.75	5.9	58.5	7.48	2.52	18.684	15.585	38.584	276	1.4	0.34	91	0.70924
11	29.5	7.7	50.1			18.729	15.63	38.744					
11.8	33	9	42.1	5.00	2.19	18.758	15.643	38.786	252	1.66	0.4	64	0.70988
12	33.5	8.5	47.3			18.653	15.658	38.833					
13.14	37.45	8.8	77.2			18.595	15.635	38.723					
13.2	37.8	8.5	77.5	9.22	3.5	18.58	15.611	38.647	277	1.79	0.5	47	0.70927
14.2	45	10.1	89.5			18.596	15.645	38.671					
15	52	9.9	90.4	11.26	3.37	18.618	15.646	38.736	300	1.88	0.57		0.71006
16.5	55.8	11.5		12.72	3.47	18.571	15.577	38.418					
16.7	56.14	11.85	73.5										
18.2	57.4	13.1	56.3	7.74	2.78	18.611	15.591	38.507	379	3.68	1.16	46	0.70880
19.3	58.5	24.6	49	9.15	1.94				317			49	0.70892
20.6	66	50	44.3	6.91	1.06	18.64	15.623	38.572	251	1.17	0.26	50	0.70841

22	68.42	27	44	7.04	1.8				280	1.61	0.41	61	0.70908
23.5	70.5	45	37	6.93	1.77				213	1.15	0.27	70	0.71143
0.23	0.26		36	4.80	0.67				171	0.48		150	0.71406
3.83	0.53		25.9	4.28	0.5	18.725	15.676	38.968	124	0.52		148	0.71673
8.31	0.87	690	34	4.40	0.86				147	0.56		148	0.71602
12.19	1.32	400	33	4.39	0.66				141	0.43		149	0.71642
18.69	2.56	180	38	5.19	0.92				142	0.54		160	0.71669
24.3	4.39		39	4.94	0.99				143	0.49		153	0.71623
25.49	5.86	68	42	5.07	1.3				148	0.48		142	0.71510
26.87	7.6	65	22.5	4.90	1.5	18.708	15.683	38.943	173	0.66	0.1	139	0.71458
28.21	9.44	57	48.5	5.00	1.7	18.699	15.689	38.97	182	0.62	0.09	138	0.71328
30.25	12.13	32	47.5	5.23	1.94				175	0.6	0.09	128	0.71250
31.69	14.03	29	51.5	5.69	2.14	18.696	15.644	38.809	205	0.86	0.17	120	0.71174
33.25	16.35	24	49.5	5.00	2.52	18.704	15.663	38.879	197	0.84	0.2	117	0.71206
33.91	17.94	20	56	5.49	2.75	18.711	15.675	38.888	213	1.23	0.3	108	0.71157
35.81	25	17	47.1	4.92	2.12	18.565	15.639	38.786	179	0.92	0.26	133	0.71264
38.09	28	18	54	5.31	1.98				159	0.89	0.19	124	0.71291
39.11	31	19	57.5	5.41	2				167	1.1	0.21	101	0.71106
40.51	34	18	53.5	6.42	2.02	18.559	15.646	38.765	177	1.02	0.2	102	0.71115
44.59	44	36	45.8	6.42	1.45	18.63	15.67	38.853	167	0.92	0.21	125	0.71356
46.01	47	37	56.5	5.79	1.89				199	1.72	0.55	99	0.71179
46.46	48	38	54.5	5.89	1.71				203	1.91	0.6	109	0.71172
47.61	51	39	42.4	5.56	1.73	18.628	15.659	38.809	229	2.15	0.67	100	0.71157
48.69	54	40	42.7	4.88	1.86	18.659	15.675	38.882	201	1.89	0.59	135	0.71258
50.65	58	45	44.5	5.27	1.64	18.664	15.646	38.779	246	1.97	0.69	136	0.71273
51.32	60	45	43	5.44	1.71	18.662	15.641	38.778	207	1.73	0.58	141	0.71323
52.83	64	47	46.6	5.22	1.74	18.642	15.609	38.696	197	1.14	0.36	135	0.71288

Appendix B

Isotope and element compositions for silicate material in LL44 GPC3 and DSDP 86 576A

Age (Ma)	$^{206}Pb/^{204}Pb$	$^{207}Pb/^{204}Pb$	$^{208}Pb/^{204}Pb$	$^{87}Sr/^{86}Sr$	Ca/Al
GPC3					
0.36	18.988	15.66	39.273	0.72230	0.030
5.35				0.72210	0.028
12.5				0.71480	0.041
17.2	18.896	15.662	39.119	0.71283	0.055
26.75					
29.5	18.961	15.636	38.969		
33	19.039	15.663	39.091	0.71192	0.058
33.5	19.014	15.662	39.122		
45	18.804	15.658	38.929		
56.14	18.809	15.65	38.846		
57.4				0.70881	0.088
66				0.70747	0.108

68.42				0.70991	0.067
70.5				0.71752	0.060
576A					
0.53	18.883	15.702	39.04	0.72058	0.038
7.6				0.71977	0.029
9.44	18.894	15.663	39.205		
16.35				0.71782	0.033
17.94	18.91	15.675	39.153		
25	18.78	15.672	39.119	0.72202	0.011
34				0.71788	0.008
44	18.797	15.673	39.108	0.72437	0.009
48				0.72449	0.005
51				0.72675	0.008
54				0.72966	0.011
64				0.72700	0.008
66					

References

Anderson, R.F., Lao, Y., Broecker, W.S., Trumbore, S.E., Hofmann, H.J., Wolfli, W., 1990. Boundary scavenging in the Pacific Ocean: a comparison of ^{10}Be and ^{231}Pa. Earth Planet. Sci. Lett. 96, 287–304.

Asahara, Y., 1999. ^{87}Sr/^{86}Sr variation in north Pacific sediments: a record of the Milankovitch cycle in the past 3 million years. Earth Planet. Sci. Lett. 171, 453–464.

Asahara, Y., Tanaka, T., Kamioka, H., Nishimura, A., 1995. Asian continental nature of ^{87}Sr/^{86}Sr ratios in north central Pacific sediments. Earth Planet. Sci. Lett. 133, 105–116.

Boyle, E.A., Chapnick, S.D., Shen, G.T., 1986. Temporal variability of lead in the western North Atlantic. J. Geophys. Res. 91, 8573–8593.

Burton, K.W., Ling, H.-F., O'Nions, R.K., 1997. Closure of the central American isthmus and its impact on North Atlantic deep-water circulation. Nature 386, 382–385.

Carpenter, R., Bennett, T.J., Peterson, M.L., 1981. 210Pb activities and fluxes to the sediments of the Washington continental slope and shelf. Geochim. Cosmochim. Acta 45, 1155–1172.

Chen, J.H., Wasserburg, G.J., von Damm, K.L., Edmond, J.M., 1987. The U–Th–Pb systematics in hot springs on the East Pacific Rise at 21°N and Guayamas Basin. Geochim. Cosmochim. Acta 50, 2467–2479.

Chow, T.J., Patterson, C.C., 1962. The occurrence and significance of lead isotopes in pelagic sediments. Geochim. Cosmochim. Acta 26, 263–308.

Christensen, J.R., Halliday, A.N., Godfrey, L.V., Hein, J.R., Rea, D.K., 1997. Climate and ocean dynamics and the lead isotopic records in Pacific ferromanganese crusts. Science 277, 913–918.

Church, S.E., 1976. The Cascade mountains revisited: a re-evaluation in light of new lead isotopic data. Earth Planet. Sci. Lett. 29, 175–188.

Corliss, B.H., Hollister, C.D., 1982. A paleoenvironmental model for Cenozoic sedimentation in the central North Pacific. In: Scrutton, R.A., Talwani, M. (Eds.), The Ocean Floor. Wiley, New York, pp. 277–304.

Cronan, D.S., 1976. Basal metalliferous sediments from the eastern Pacific. Geol. Soc. Am. Bull. 87, 928–934.

Dasch, E.J., 1981. Lead isotopic composition of metalliferous sediments from the Nazca plate. GSA Mem. 154, 199–209.

Doyle, P.S., 1980. Seabed disposal program: improvement of ichthyolith stratigraphy for giant piston core 3. Progress Report for Sandia Laboratories.

Doyle, P.S., Riedel, W.R., 1979. Cretaceous to Neogene ichthyoliths in a giant piston core from the central North Pacific. Micropaleontology 25, 337–364.

Doyle, P.S., Riedel, W.R., 1985. Ichthyolith biostratigraphy of western North Pacific pelagic clays, Deep Sea Drilling Project Leg 86. Init. Repts. DSDP 86. US Govt. Printing Office, pp. 349–366.

Elbaz-Poulichet, F., Hollinger, P., Huang, W.W., Martin, J.M., 1984. Lead cycling in estuaries, illustrated by the Gironde estuary, France. Nature 308, 409–414.

Flegal, A.R., Itoh, K., Patterson, C.C., Wong, C.S., 1986. Vertical profile of lead isotopic compositions in the north-east Pacific. Nature 321, 689–690.

Frank, M., Reynolds, B.C., O'Nions, R.K., 1999. Nd and Pb isotopes in Atlantic and Pacific water masses before and after closure of the Panama gateway. Geology 27, 1147–1150.

Godfrey, L.V., Mills, R.A., Elderfield, H., Gurvich, E., 1994. Lead behaviour at the TAG hydrothermal vent field, 26°N, Mid-Atlantic Ridge. Mar. Chem. 46, 237–254.

Hamelin, B., Grousset, F., Scholkovitz, E.R., 1990. Pb isotopes in surficial pelagic sediments from the North Atlantic. Geochim. Cosmochim. Acta 54, 37–47.

Hegner, E., Tatsumoto, M., 1987. Pb, Sr, and Nd isotopes in basalts and sulfides from the Juan de Fuca Ridge. J. Geophys. Res. 92, 11380–11386.

Hemming, S.R., McLennan, S.M., 2001. Pb isotope compositions of modern deep sea turbidites. Earth Planet. Sci. Lett. 184, 489–503.

Hess, J., Bender, M.L., Schilling, J.-G., 1986. Evolution of the ratio of strontium-87 to strontium-86 in seawater from Cretaceous to present. Science 231, 979–984.

Ito, E., White, W.M., Göpel, C., 1987. The O, Sr, Nd and Pb isotopes geochemistry or MORB. Chem. Geol. 62, 157–176.

Janecek, T.R., 1985. Eolian sedimentation in the northwest Pacific Ocean: a preliminary examination of the data from Deep-Sea Drilling Project sites 565 and 578. Init. Repts. DSDP 86. US Govt. Printing Office, pp. 589–603.

Jones, C.E., Halliday, A.N., Rea, D.K., Owen, R.M., 2000. Eolian inputs of lead to the North Pacific. Geochim. Cosmochim. Acta 64, 1405–1416.

Keith, S.B., 1978. Paleosubduction geometries inferred from Cretaceous and Tertiary magmatic patterns in southwest North America. Geology 6, 516–521.

Koschinsky, A., Halbach, P., 1995. Sequential leaching of marine ferromanganese precipitates: genetic implications. Geochim. Cosmochim. Acta 59, 5113–5132.

Koschinsky, A., Stascheit, A., Bau, M., Halbach, P., 1997. Effects of phosphatization on the geochemical and mineralogical composition of marine ferromanganese crusts. Geochim. Cosmochim. Acta 61, 4079–4094.

Kyte, F.T., Wasson, J.T., 1986. Accretion rate of extraterrestrial matter: iridium deposited 33 to 67 million years ago. Science 232, 1225–1229.

Kyte, F.T., Leinen, M., Heath, G.R., Zhou, L., 1993. Cenozoic sedimentation history of the central North Pacific: inferences from the elemental geochemistry of core LL44-GPC3. Geochim. Cosmochim. Acta 57, 1719–1740.

Leinen, M., 1985. Quartz content of northwest Pacific Hole 576A and implications for Cenozoic eolian transport. Init. Repts. DSDP 86. US Govt. Printing Office, pp. 581–588.

Leinen, M., 1987. The origin of paleochemical signatures in north Pacific pelagic clays: partitioning experiments. Geochim. Cosmochim. Acta 51, 305–319.

Leinen, M., Heath, G.R., 1981. Sedimentary indicators of atmospheric activity in the northern hemisphere during the Cenozoic. Palaeogeogr., Palaeoclimatol., Palaeoecol. 36, 1–21.

Ling, H.F., Burton, K.W., O'Nions, R.K., Kamber, B.S., von Blanckenburg, F., Gibb, A.J., Hein, J.R., 1997. Evolution of Nd and Pb isotopes in Central Pacific seawater from ferromanganese crusts. Earth Planet. Sci. Lett. 146, 1–12.

Milliman, J.D., Syvitski, J.P.M., 1992. Geomorphic/tectonic control of sediment discharge to the oceans; the importance of small mountainous rivers. J. Geol. 100, 525–544.

O'Nions, R.K., Frank, FM., von Blanckenburg, F., Ling, H.-F., 1998. Secular variation of Nd and Pb isotopes in ferromanganese crusts from the Atlantic, Indian and Pacific Oceans. Earth Planet. Sci. Lett. 155, 15–28.

Nakai, S., Halliday, A.N., Rea, D.K., 1993. Provenance of dust in the Pacific Ocean. Earth Planet. Sci. Lett. 119, 143–157.

Peucker-Ehrenbrink, B., Ravizza, G., Hofmann, A.W., 1995. The marine $^{187}Os/^{186}Os$ record of the past 80 million years. Earth Planet. Sci. Lett. 130, 155–167.

Rea, D.K., 1994. The paleoclimatic record provided by eolian deposition in the deep-sea—The geologic history of the wind. Rev. Geophys. 32, 159–195.

Rea, D.K., Janecek, T.R., 1982. Late Cenozoic changes in atmospheric circulation deduced from North Pacific eolian sediments. Mar. Chem. 49, 149–167.

Reynolds, B.C., Frank, M., O'Nions, R.K., 1999. Nd- and Pb-isotope time series from Atlantic ferromanganese crusts: implications for changes in provenance and paleocirculation over the last 8 Myr. Earth Planet. Sci. Lett. 173, 381–396.

Schaule, B.K., Patterson, C.C., 1981. Lead concentrations in the northeast Pacific: evidence for global anthropogenic perturbations. Earth Planet. Sci. Lett. 54, 97–116.

Schramm, C.T., 1989. Cenozoic climate variation recorded by quartz and clay minerals in North Pacific sediments. In: Leinen, M., Sarnthein, M. (Eds.), Paleoclimatology and Paleometerology: Modern and Past Patterns of Global Atmospheric Transport; NATO ASI Series, vol. 282. Kluwer Academic Publishing, Dordrecht, pp. 805–839.

Sherrell, R.M., Boyle, E.A., Hamelin, B., 1992. Isotopic equilibration between dissolved and suspended particulate lead in the Atlantic Ocean: evidence from ^{210}Pb and stable Pb isotopes. J. Geophys. Res. 97, 11257–11268.

Straub, S.M., Schmincke, H.U., 1998. Evaluating the tephra input into Pacific Ocean sediments: distribution in space and time. Geol. Rundsch. 87, 461–476.

Sun, S.-S., 1980. Lead isotopic study of young volcanic rocks from mid-ocean ridges, ocean islands and island arcs. Philos. Trans. R. Soc. London, Ser. A 297, 409–445.

Van Andel, T.J., Heath, G.R., Moore Jr., T.C. 1975. Cenozoic history and paleoceanography of the Central Equatorial Pacific. GSA Mem. 143, 143 pp.

von Blanckenburg, F., Igel, H., 1999. Lateral mixing and advection of reactive isotope tracers in ocean basins: observations and mechanisms. Earth Planet. Sci. Lett. 169, 113–128.

von Blanckenburg, F., O'Nions, R.K., Hein, J.R., 1996. Distribution and sources of pre-anthropogenic lead isotopes in deep ocean water from Fe–Mn crusts. Geochim. Cosmochim. Acta 60, 4957–4963.